Nonlinear Magneto-optical Rotation via Alignment-to-Orientation Conversion

D. Budker,[1,2,*] D. F. Kimball,[1] S. M. Rochester,[1] and V. V. Yashchuk[1]

[1]*Department of Physics, University of California at Berkeley, Berkeley, California 94720-7300*
[2]*Nuclear Science Division, Lawrence Berkeley National Laboratory, Berkeley, California 94720*

(Received 10 March 2000)

Nonlinear magneto-optical rotation is investigated at high light powers where the rotation is significantly modified by ac Stark shifts. These shifts are shown to change the overall sign of rotation for closed $F \rightarrow F + 1$ transitions compared to the low light power limit. The effect is demonstrated by measurements in rubidium and density matrix calculations. The results are important for applications of nonlinear optical rotation such as sensitive magnetometry.

PACS numbers: 32.60.+i, 32.80.Bx, 42.50.Gy, 42.50.Hz

Nonlinear magneto-optical rotation (NMOR) arises when sufficiently intense light interacts with atoms in the presence of a magnetic field [1,2]. Recently, two approaches to NMOR-based magnetometry have been pursued, one involving ultranarrow (1 Hz) resonances [3,4], and the other using high density atomic samples [5]. The optimum sensitivity in both approaches is achieved for light powers where the number of optical pumping cycles during the relaxation time of ground state coherences exceeds unity. Here we show that under such conditions the dominant physical mechanism causing NMOR can be quite different from that in the low light power regime (quantitatively described by a perturbative model [6]). In particular, we show that alignment-to-orientation conversion [7–12] due to the combined action of the magnetic field and optical electric field is the primary mechanism responsible for NMOR at the light frequencies and intensities where the highest sensitivity to magnetic fields is achieved [4].

In this work we investigate nonlinear magneto-optic effects related to the evolution of atomic polarization moments (the coherence effects) in the Faraday geometry, where the magnetic field is oriented along the propagation direction of linearly polarized light (Fig. 1). For low light intensities, analytic expressions can be derived which describe the coherence effects in terms of a three stage process [3,6]: (1) atoms are optically pumped into an aligned state, causing the vapor to acquire linear dichroism, (2) the atomic alignment precesses in the magnetic field, rotating the axis of dichroism, and (3) the light polarization is rotated by interaction with the dichroic atomic medium, since the alignment is no longer along the direction of light polarization. This model predicts that for closed transitions, the sign of NMOR for $F \rightarrow F - 1, F$ transitions (F is the total angular momentum in the lower state) should be opposite to the sign of optical rotation for $F \rightarrow F + 1$ transitions [13]. This is in agreement with measurements at relatively low light intensities [2,3,6]. However, as light power is increased, we have observed that NMOR for closed $F \rightarrow F + 1$ transitions changes sign, indicating that a different physical mechanism becomes dominant.

Figure 2 shows experimental and theoretical [14] NMOR spectra for the ^{85}Rb $F = 3 \rightarrow F'$ and ^{87}Rb $F = 2 \rightarrow F'$ hyperfine components of the $D2$ line (780 nm) for two different light powers. Note that the signs of rotation for the ^{87}Rb $F = 2 \rightarrow 3$ and ^{85}Rb $F = 3 \rightarrow 4$ components reverse at the higher light power.

In order to illustrate the mechanisms responsible for this effect, let us consider the simpler cases of closed, spectrally isolated $1 \rightarrow 0$ and $1 \rightarrow 2$ transitions with separated pump, precession, and probe regions (Fig. 3). This scheme is similar to that employed in recent NMOR experiments with separated fields [15]. In our calculations, the pump light frequency is held fixed on resonance and its power corresponds to the optical pumping saturation parameter $\kappa = d^2 E_0^2/(\gamma_0 \gamma_t) \approx 1$, where d is the transition dipole moment, E_0 is the amplitude of the light electric field, γ_0 is the homogeneous width of the transition, and γ_t is the inverse of the transit time through each of the regions. The probe light power corresponds to $\kappa \ll 1$. In the precession region there is a $\hat{z}$-directed magnetic field of magnitude $B_z \ll \gamma_t/(2 g_F \mu)$ where g_F is the ground state Landé factor and μ is the Bohr magneton. An $\hat{x}$-directed dc electric field is introduced to model the effect of the optical field on precession of atomic polarization.

Figure 4 shows the calculated frequency dependence of NMOR. Also shown are the symmetric and antisymmetric (with respect to probe detuning) contributions to the rotation. The symmetric contribution has a frequency dependence characteristic of the imaginary part of the refractive

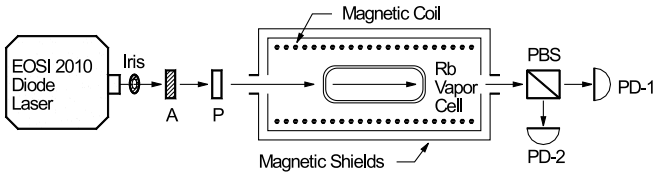

FIG. 1. Schematic diagram of experimental setup. The laser is an external cavity diode laser (EOSI 2010). The uncoated cylindrical glass vapor cell contains a natural isotopic mixture of Rb. A—attenuator; P—linear polarizer; PBS—polarizing beam splitter used to measure polarization rotation; PD-1,2—photodiodes.

 0031-9007/00/85(10)/2088(4)$15.00

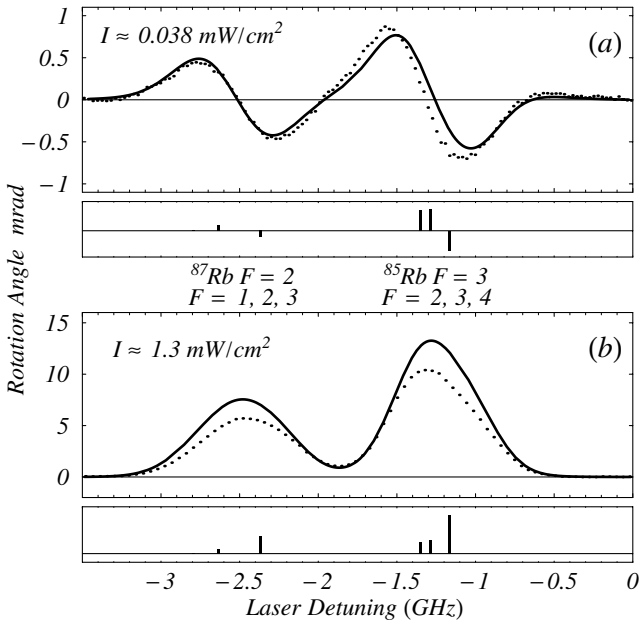

FIG. 2. Comparison of experimental NMOR spectra to density matrix calculations. Dots—data points; solid curves—theory (without free parameters). Offset vertical bars indicate the central frequencies and calculated relative contributions of different hyperfine components ($F \rightarrow F'$) to the overall rotation. Laser detuning is relative to the $D2$ line center. Magnetic field is $\approx$0.1 G (where NMOR is relatively large and coherence effects dominate), laser beam diameter is $\approx$3.5 mm, and Rb density is $\sim 10^{10}$ atoms/cm^3. Residual discrepancies between data and theory may be due to nonuniform spatial distribution of light intensity.

index and is related to linear dichroism. The antisymmetric contribution, which appears only when there is an electric field in the precession region, behaves as the real part of the refractive index and is the effect of circular birefringence. The appearance of circular birefringence implies that atomic orientation along the $\hat{z}$ direction is created in the precession region.

The conversion of the atomic alignment produced in the pump region into orientation can be understood in the following way (see, e.g., Refs. [11,12]). The electric field $\vec{E}_s$ induces a net ground state dipole moment $\vec{d}_{ind} = \overleftrightarrow{\alpha} \cdot \vec{E}_s$,

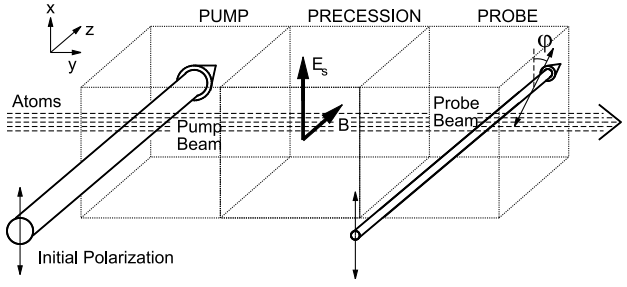

FIG. 3. Schematic diagram of an experiment with separated pump, precession, and probe regions. Atoms move with constant velocity in the $\hat{y}$ direction.

where $\overleftrightarrow{\alpha}$ is the polarizability tensor. For polarized atoms, $\vec{d}_{ind}$ acquires a component $\propto \overleftrightarrow{Q} \cdot \vec{E}_s$, where $\overleftrightarrow{Q}$ is the ground state quadrupole moment. In general, if the axis of alignment is neither parallel nor perpendicular to the electric field, $\overleftrightarrow{Q} \cdot \vec{E}_s$ will not be along $\vec{E}_s$. The electric field then creates orientation via the $\vec{d}_{ind} \times \vec{E}_s$ torque, as experimentally demonstrated, e.g., in Refs. [8,11]. In our case, since the axis of alignment produced by optical pumping is along $\vec{E}_s$, no orientation is generated in the precession region by the action of the electric field alone. However, the magnetic field $\vec{B}$ causes alignment to precess about $\hat{z}$ at the Larmor frequency Ω_L, so the alignment axis is no longer along the electric field. For small magnetic fields ($\Omega_L \ll \gamma_t$), the component of $\vec{d}_{ind}$ orthogonal to the electric field is proportional to $(\vec{B} \times \overleftrightarrow{Q}_i) \cdot \vec{E}_s$ ($\overleftrightarrow{Q}_i$ is the quadrupole moment produced in the pump region). The induced orientation $\vec{O}$ for small electric and magnetic fields is thus described by

$$\vec{O} \propto \vec{d}_{ind} \times \vec{E}_s \propto (\vec{B} \times \overleftrightarrow{Q}_i) \cdot \vec{E}_s \times \vec{E}_s \,. \qquad (1)$$

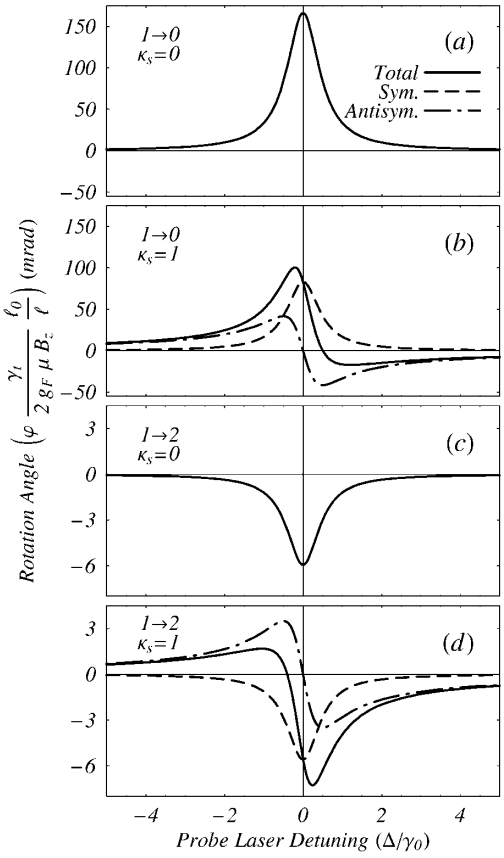

FIG. 4. Calculated Doppler-free optical rotation spectra for separated pump, precession, and probe fields. $\Delta \equiv \omega_L - \omega_0$, ω_0 is the resonance frequency of the transition, and ω_L is the probe light frequency; l/l_0 is the number of unsaturated absorption lengths; $\kappa_s = d^2 E_s^2/(\omega_0 \gamma_t)$. The maximum rotation angle obtained for the $1 \rightarrow 2$ transition is smaller than that for the $1 \rightarrow 0$ case because of less efficient alignment creation via optical pumping and a reduced effect of ground state polarization on absorption and refraction.

It can be shown that the sign of the quadrupole moment produced by optical pumping is opposite for $1 \rightarrow 2$ and $1 \rightarrow 0$ transitions, therefore $\vec{O}$ is of opposite sign for the two cases. For a given $\vec{O}$, the rotation of probe light polarization for a $1 \rightarrow 2$ transition is of opposite sign to that for a $1 \rightarrow 0$ transition. This is because opposite circular polarizations have stronger interactions with a given oriented atomic sample for the two transitions. Thus, for a given probe beam frequency, NMOR due to the induced circular birefringence is of the same overall sign for both transitions (Fig. 4).

Figure 5 shows the results of density matrix calculations for NMOR with separated regions as a function of the parameter $\kappa_s = d^2 E_s^2/(\omega_0 \gamma_t)$, which characterizes the Stark shift due to the static electric field. For $\kappa_s \ll 1$, NMOR related to circular birefringence is linear in κ_s, as expected from Eq. (1). For large values of κ_s, the birefringence effect dominates. Since linear dichroism and circular birefringence produce rotation of opposite signs in the case of the $1 \rightarrow 2$ transition (for probe detuning $\Delta < 0$), the overall sign of the NMOR flips when Stark-induced birefringence becomes the dominant cause of the rotation.

Now we consider a single region where there is no dc electric field and a single light beam serves as both pump and probe. Here, alignment-to-orientation conversion can occur due to ac Stark shifts Δ_{ac} produced by the electric field of the light. Figure 6 shows NMOR spectra for this case. There are several factors that contribute to the frequency dependence of optical rotation. The optical electric field $\vec{E}_l$ induces a ground state dipole moment $\vec{d}_{ind}$ which oscillates at the light frequency. Again, the component of $\vec{d}_{ind}$ orthogonal to $\vec{E}_l$ is proportional to the optically pumped quadrupole moment, whose amplitude has a detuning dependence given by a Lorentzian function. The phase of $\vec{d}_{ind}$ with respect to $\vec{E}_l$ and its amplitude (for a given quadrupole moment) also depend on detuning. Because of these factors, the induced orientation has a frequency dependence proportional to the product of the Lorentzian function describing optical pumping and a dispersive function describing the orientation produced by the $\vec{d}_{ind} \times \vec{E}_l$ torque for a given alignment. The dispersive function is proportional to Δ_{ac}, which for the Doppler-free case with $dE_0 < \gamma_0$ is given by [16]

$$\Delta_{\mathrm{ac}} \approx \frac{d^2 E_0^2 (\omega_L - \omega_0)}{4(\omega_L - \omega_0)^2 + \gamma_0^2}. \qquad (2)$$

Note that, in contrast to the case of separated fields and dc Stark shifts discussed earlier, in this case the contribution from ac Stark-induced circular birefringence is symmetric with respect to detuning (Fig. 6). This is because NMOR due to circular birefringence is described by a product of two antisymmetric functions. One describes the induced orientation and the other describes the rotation angle produced by a given orientation (proportional to the real part of the refractive index, as in Fig. 4). Also note that in the $1 \rightarrow 2$ case, rotation due to circular birefringence and rotation due to linear dichroism have opposite signs.

In order to describe experimental data, Doppler-free NMOR spectra must be convolved with the atomic velocity distribution. Calculations indicate that at high light powers in the presence of Doppler broadening, NMOR due to circular birefringence dominates for all detunings. This is the regime where NMOR-based magnetometers achieve optimum sensitivity [4,5]. For closed $F \rightarrow F + 1$ transitions, this effect causes the overall rotation to flip sign, as observed in the experimental data (Fig. 2).

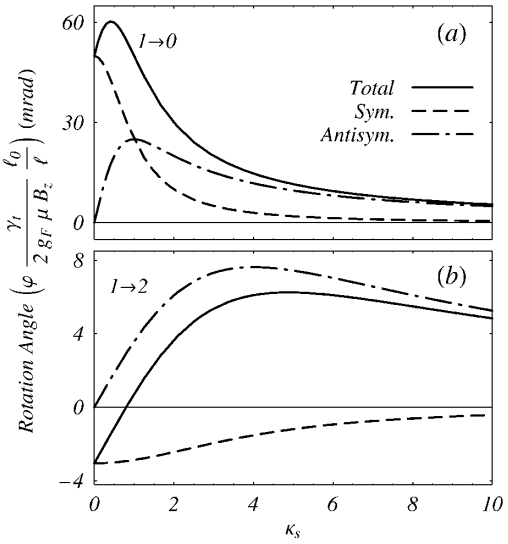

FIG. 5. Calculated Doppler-free optical rotation of probe light as a function of κ_s for separated pump, precession, and probe fields. Probe light is detuned by $\Delta = -\gamma_0/2$. Note the sign change of the overall rotation for the $1 \rightarrow 2$ case as the electric field is increased.

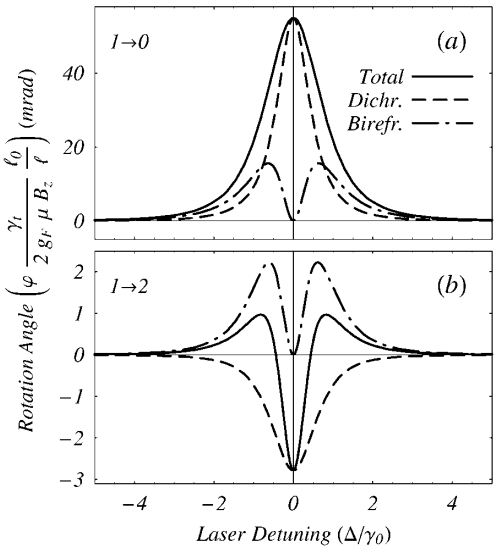

FIG. 6. Calculated Doppler-free optical rotation in an experimental setup similar to that of Fig. 1, with $\kappa = 5$. Plots show overall rotation, NMOR due to linear dichroism, and NMOR related to ac Stark-induced circular birefringence.

Here we have shown that ac Stark shifts caused by the optical electric field play an important role in the evolution of atomic polarization in the presence of a magnetic field, leading to optical rotation. Even in the absence of a magnetic field, similar effects can cause nonlinear optical rotation and induce ellipticity. For example, evolution of atomic polarization (e.g., orientation-to-alignment conversion) in an elliptically polarized optical electric field can cause self-rotation of light polarization [17]. If an electric field is applied at an angle to the directions of light propagation and linear polarization, Stark shifts can modify optical properties of the medium. Such effects can be applied in atomic spectroscopy (e.g., measurements of electric polarizabilities [11]) and electromagnetic field measurements [18].

Alignment-to-orientation conversion can also significantly modify the experimental signature of nonlinear optical rotation caused by permanent atomic electric dipole moments (EDMs) [4,15,19]. The effect of an EDM in the presence of a static electric field on the evolution of atomic polarization is equivalent to that of a weak magnetic field (in the direction of the electric field). Therefore, at high light powers, where optimum shot-noise-limited sensitivity to an EDM is achieved [4], the optical electric field will convert alignment into orientation via mechanisms described above. For closed $F \rightarrow F + 1$ transitions, this changes the sign of the rotation produced by an EDM. In addition, the effects of alignment-to-orientation conversion caused by both optical and static fields should be taken into account in the analysis of systematic errors.

In conclusion, we have considered alignment-to-orientation conversion in NMOR, which causes optical rotation via circular birefringence. This effect dominates at high light powers ($\kappa \gg 1$). It explains a reversal of the sign of rotation for closed $F \rightarrow F + 1$ transitions observed in experiments. These results are important for sensitive magnetometry and other applications.

The authors thank M. Zolotorev and A. I. Okunevich for fruitful discussions. This research is supported by the Office of Naval Research, Grant No. N00014-97-1-0214.

*Email address: budker@socrates.berkeley.edu

[1] W. Gawlik, in *Modern Nonlinear Optics,* edited by M. Evans and S. Kielich, Advances in Chemical Physics Series Vol. LXXXV (Wiley, New York, 1994), Pt. 3.

[2] D. Budker, D. J. Orlando, and V. Yashchuk, Am. J. Phys. **67**, 584 (1999).

[3] D. Budker, V. Yashchuk, and M. Zolotorev, Phys. Rev. Lett. **81**, 5788 (1998).

[4] V. Yashchuk, D. Budker, and M. Zolotorev, in *Trapped Charged Particles and Fundamental Physics,* edited by D. H. E. Dubin and D. Schneider (American Institute of Physics, New York, 1999), pp. 177–181.

[5] V. A. Sautenkov, M. D. Lukin, C. J. Bednar, I. Novikova, E. Mikhailov, M. Fleischhauer, V. L. Velichansky, G. R. Welch, and M. O. Scully, Phys. Rev. A **62**, 023810 (2000); M. Fleischhauer, A. B. Matsko, and M. O. Scully, Phys. Rev. A **62**, 013808 (2000).

[6] S. I. Kanorsky, A. Weis, J. Wurster, and T. W. Hänsch, Phys. Rev. A **47**, 1220 (1993).

[7] Here alignment designates the second (quadrupole) polarization moment, and orientation designates the first (dipole) polarization moment; see E. B. Alexandrov, M. P. Chaika, and G. I. Kvostenko, *Interference of Atomic States* (Springer-Verlag, Berlin, 1993).

[8] M. Lombardi, J. Physique **30**, 631 (1969).

[9] C. Cohen-Tannoudji and J. Dupont-Roc, Opt. Commun. **1**, 184 (1969).

[10] M. Pinard and C. G. Aminoff, J. Phys. **43**, 1327 (1982).

[11] R. C. Hilborn, L. R. Hunter, K. Johnson, S. K. Peck, A. Spencer, and J. Watson, Phys. Rev. A **50**, 2467 (1994).

[12] R. C. Hilborn, Am. J. Phys. **63**, 330 (1995).

[13] This is because for closed transitions, the axis of dichroism corresponding to smaller absorption is initially parallel to the direction of the pump light polarization for $F \rightarrow F - 1, F$ transitions (atoms are pumped into a dark state), and perpendicular to the pump light polarization for $F \rightarrow F + 1$ transitions (atoms are pumped into a bright state with greater absorption compared to the unpolarized state [A. P. Kazantsev, V. S. Smirnov, A. M. Tumaikin, and I. A. Yagofarov, Opt. Spectrosc. (USSR) **57**, 116 (1984)]).

[14] In our calculations, a density matrix is written for Zeeman sublevels of each ground state hyperfine level and for those of all the excited states accessible via optical transitions from this hyperfine level. The effects of repopulation pumping are included in the calculations. These calculations are based on principles similar to those applied in M. G. Kozlov, Opt. Spectrosc. (USSR) **67**, 789 (1989); S. V. Fomichev, J. Phys. B **24**, 4695 (1991); G. Nienhuis and F. Schuller, Opt. Commun. **151**, 40 (1998), and references therein.

[15] B. Schuh, S. I. Kanorsky, A. Weis, and T. W. Hänsch, Opt. Commun. **100**, 451 (1993).

[16] Under the stated conditions, this formula is a good approximation of the expression obtained from dressed state considerations for a two-level atom in, e.g., C. Cohen-Tannoudji, Metrologia **13**, 161 (1977).

[17] D. Budker, R. Y. Chiao, D. S. Hsiung, S. M. Rochester, and V. V. Yashchuk, in *Quantum Electronics and Laser Science,* OSA Technical Digest (Optical Society of America, Washington, D.C., 2000), p. 252.

[18] D. Budker, D. F. Kimball, S. M. Rochester, and V. V. Yashchuk, Report No. LBNL PUB-5453, 1999.

[19] L. M. Barkov, M. S. Zolotorev, and D. Melik-Pashayev, Sov. JETP Pis'ma **48**, 144 (1988); L. M. Barkov, D. A. Melik-Pashayev, and M. S. Zolotorev, Opt. Commun. **70**, 467 (1989).